

This discussion paper is/has been under review for the journal *Climate of the Past* (CP).
Please refer to the corresponding final paper in CP if available.

Using ice-flow models to evaluate potential sites of million year-old ice in Antarctica

B. Van Liefferinge and F. Pattyn

Laboratoire de Glaciologie, Université Libre de Bruxelles, CP 160/03,
Avenue F. D. Roosevelt 50, 1050 Brussels, Belgium

Received: 30 April 2013 – Accepted: 7 May 2013 – Published: 28 May 2013

Correspondence to: B. Van Liefferinge (bvlieffe@ulb.ac.be)

Published by Copernicus Publications on behalf of the European Geosciences Union.

2859

Abstract

Finding suitable potential sites for an undisturbed record of million-year old ice in Antarctica requires a slow-moving ice sheet (preferably an ice divide) and basal conditions that are not disturbed by large topographic variations. Furthermore, ice should be thick and cold basal conditions should prevail, since basal melting would destroy the bottom layers. However, thick ice (needed to resolve the signal at sufficient high resolution) increases basal temperatures, which is a conflicting condition in view of finding a suitable drill site. In addition, slow moving areas in the center of ice sheets are also low-accumulation areas, and low accumulation reduces potential cooling of the ice through vertical advection. While boundary conditions such as ice thickness and accumulation rates are relatively well constraint, the major uncertainty in determining basal conditions resides in the geothermal heat flow (GHF) underneath the ice sheet. We explore uncertainties in existing GHF datasets and their effect on basal temperatures of the Antarctic ice sheet and propose an updated method based on Pattyn (2010) to improve existing GHF datasets in agreement with known basal temperatures and their gradients to reduce this uncertainty. Both complementary methods lead to a better comprehension of basal temperature sensitivity and a characterization of potential ice coring sites within these uncertainties.

1 Introduction

One of the major future challenges in the ice coring community is the search for a continuous and undisturbed ice core record dating back to 1.5 million years BP (Jouzel and Masson-Delmotte, 2010). The reason for such quest is that the oldest part of the EPICA Dome C ice core has revealed low values of CO₂ from 650 000 to 800 000 yr ago (Lüthi et al., 2008), which questions the strong Antarctic temperature-carbon cycle coupling on long time scales. Marine records show evidence of a reorganisation of the pattern of climate variability around 1 Myr ago, shifting from the “obliquity” dominated

2860

signal, characterized by 40 000 yr weak glacial-interglacial cycles to the “eccentricity”-dominated signal with longer glacial-interglacial cycles (Lisiecki and Raymo, 2005). The origin of this major climate reorganization (the so-called Mid-Pleistocene Transition, MPT) remains unknown and may be intrinsic to a series of feedback mechanisms between climate, cryosphere and carbon cycle (Jouzel and Masson-Delmotte, 2010).
5 Alternatively, a recent study has demonstrated that climate oscillations over the past four million years can be explained by a single mechanism, i.e. the synchronization of nonlinear internal climate oscillations and the 413 000 yr eccentricity cycle (Rial et al., 2013). According to model calculations in conjunction with spectral analysis, Rial et al.
10 (2013) find that the climate system first synchronized to this 413 000 yr eccentricity cycle about 1.2 million years ago, roughly coinciding with this MPT.

Deep ice core drillings have been carried out in the past in Antarctica, reaching back in time over several hundred thousands of years. Amongst the longest records are Vostok (Petit et al., 1999), EPICA Dome Concordia (EPICA community members, 2004),
15 Dome Fuji (Watanabe et al., 2003), and EPICA Dronning Maud Land (EPICA community members, 2006). The longest record is EPICA Dome Concordia, going back for more than 800 000 yr. Those records have in common that they are all recovered in the center of the ice sheet, and given the fact that the Antarctic ice sheet has been relatively constant in size and over the last 13 million years (DeConto and Pollard, 2003), they are consequently undisturbed by dramatic changes in ice flow, contrary to the longest
20 records from the Greenland ice sheet (Johnson, 2001; NEEM community members, 2013).

In theory, and in absence of basal melting, these deep Antarctic records could reach several million years back in time with layers getting infinitesimally thin near the bottom.
25 In reality, however, all deep records lack the bottom sequence as they are all found to be at pressure melting point and lower layers are melted away or heavily disturbed due to complex basal processes. Furthermore, resolving deep records not only requires that the bottom sequence is unaltered, but that the ice is sufficiently thick so that the gas

2861

signal can still be retrieved and analyzed with sufficient high resolution in the bottom layers.

In this paper we use several thermodynamic models to infer suitable areas for retrieving long ice-core records. We first investigate the most influential parameters having an effect on ice-core record length. Secondly, we apply this simple concept to evaluate
5 uncertainties in GHF and use this uncertainty to guide the search for a suitable drilling place. Thirdly, we carry out a sensitivity analysis with a three-dimensional thermodynamical model (Pattyn, 2010) to determine the sensitivity of basal conditions to uncertainties in GHF, guided by a priori knowledge of basal conditions through the
10 geographical distribution of subglacial lakes. Results are discussed in the last section.

2 Why obvious drill sites are unsuitable

Obvious places to look for oldest ice are the deepest parts of the ice sheet, where ice is thick, and accumulation rates are low. However, a thick ice cover insulates very well and keeps the geothermal heat from escaping to the surface. Furthermore, we know
15 that at least 379 subglacial lakes exist under the Antarctic ice sheet, which implies that large portions of the bedrock should be at pressure melting point (Smith et al., 2009; Pattyn, 2010; Wright and Siegert, 2012). Most subglacial lakes occur in the so-called Lakes District (stretching between Subglacial Lake Vostok and Wilkes Land in East Antarctica), characterized by a thick ice cover and also low geothermal heat flow
20 (Shapiro and Ritzwoller, 2004; Pollard et al., 2005). Therefore, GHF is not the main culprit in causing subglacial melt.

The interplay between GHF and accumulation rates is very subtle, as high GHF increases basal temperatures, while high accumulation rates cool down the ice mass. To illustrate this we calculate the minimum GHF needed to reach pressure melting point at
25 the bottom of any ice mass as a function of environmental parameters. This can easily be determined analytically (Hindmarsh, 1999; Siegert, 2000). Using the simplified

2862

with

$$q_s = -H \int_b^s \mathbf{v}_H(z') dz', \quad (5)$$

and where b and s are the bottom and the surface of the ice sheet (m a.s.l.), respectively. Integrating Eq. (4) over the whole surface of the ice sheet, starting at the ice divides, one obtains the vertically averaged horizontal balance velocities $\bar{\mathbf{v}}_H = (\bar{v}_x, \bar{v}_y)$. Details of this procedure are given in Pattyn (2010).

Using the above datasets, the minimum geothermal heat flow G_{\min} from Eq. (1) needed to reach pressure melting point at the bed is calculated for the areas of the Antarctic ice sheet where horizontal flow velocities are $< 2 \text{ myr}^{-1}$ and where ice thickness $H > 2000 \text{ m}$. This ice thickness is considered to be the lower limit for possibly recovery of a million-year old climate signal (H. Fischer, personal communication, 2013). The calculated values of G_{\min} are subsequently compared to known values of GHF.

Several datasets of derived GHF underneath the Antarctic ice sheet exist. The first one (G_1) uses a global seismic model of the crust and the upper mantle to guide the extrapolation of existing heat-flow measurements to regions where such measurements are rare or absent (Shapiro and Ritzwoller, 2004). The second GHF database (G_2) stems from satellite magnetic measurements (Fox-Maule et al., 2005). Values of GHF are in the same range as Shapiro and Ritzwoller (2004), but the spatial variability is contrasting. Heat flow measurements according to Fox-Maule et al. (2005) are also considerably higher than those by Shapiro and Ritzwoller (2004). A third dataset is due to Puruker (2013). This geothermal heat flux data set (G_3) is based on low resolution observations collected by the CHAMP satellite between 2000 and 2010, and produced from the MF-6 model following the technique described in Fox-Maule et al. (2005). While the technique is similar, GHF values are considerably lower than the latter, and even lower than those derived from the seismic model (Shapiro and Ritzwoller, 2004).

2865

3.2 Results

In view of the large uncertainty in GHF estimates, we combined all three datasets into two databases, i.e. a mean GHF, \bar{G} , and a standard deviation, σ_G . The latter is calculated based on the inter-database variability and the standard deviation given for the Shapiro and Ritzwoller (2004) dataset in the following way:

$$\sigma_G = \sigma [G_1 - \sigma(G_1), G_1 + \sigma(G_1), G_2, G_3]. \quad (6)$$

Both are depicted in Fig. 2. High values of σ_G indicate a large dispersion between the three datasets. These are essentially found in West Antarctica and along the Transantarctic Mountains. The lowest values are restricted to the central parts of the East-Antarctic continent.

The calculated values of G_{\min} are directly compared to the map of mean GHF. For $G_{\min} < \bar{G}$, the observed GHF is too elevated to prevent the bottom ice to reach pressure melting and most likely (within error bounds) the ice is temperate. For $G_{\min} > \bar{G}$ the minimum GHF needed to reach pressure melting at the base is higher than the value reported. Of course, this information needs to be further evaluated against the dispersion between the GHF datasets, represented by σ_G . The result is shown in Fig. 3, where the rectangular area points to the potentially most suitable conditions in terms of basal temperature, i.e. the largest difference between actual GHF and minimum GHF in combination with the lowest variability between the three GHF datasets. The furthest to the right in Fig. 3, the colder the bed because a significant higher GHF than observed is needed to make the bed temperate; the lower the value of σ_G , the more likely there is a small spread (hence reduced uncertainty) in GHF, so that the observed value is likely. On top of this, the color scale shows the ice thickness for each of the points. The thickest ice is obviously corresponding to zones that are temperate (negative values of ΔG), while for large positive ΔG and small σ_G , ice is also the thinnest.

These restrictions (superposed on the ice flow speed limit and minimum ice thickness) lead to a few areas in the central part of the Antarctic ice sheet that are

2866

lakes. Both regions are characterized by relatively low basal temperatures (Fig. 5) and are unlikely to reach pressure melting point, despite the large RMSE due to – mainly – differences between the GHF datasets.

6 Discussion and conclusions

5 Since both the simple and ensemble model results are complementary (but not totally independent) in nature, they can be combined to form a joint dataset. The analysis is limited to flow speeds lower than 2 myr^{-1} and ice thickness $H > 2000 \text{ m}$, which are considered as suitable conditions for retrieving and resolving ice older than one million years. Given the uncertainty in GHF originating from the large dispersion between the
10 different datasets (both spatially and in terms of absolute values), we put constraints on the selection of suitable sites: (i) the minimum GHF needed to reach pressure melting point should at least be 5 mW m^{-2} higher than the mean value from the combined GHF datasets; (ii) the variability between the GHF datasets for a given site expressed by the standard deviation σ_G should equally be less than 25 mW m^{-2} ; (iii) the mean basal
15 temperature according to the ensemble model calculations should be less than $-5 \text{ }^\circ\text{C}$ (but lower values are favored). Results are displayed in Fig. 7. We explored different values for these constraints, but the general pattern remains the same. The main effect is the stronger the constraint, the smaller the areas, but the geographical distribution is not altered.

20 Due to the velocity and ice thickness constraints, all sites are situated near the ice divides. Not surprisingly, areas near the major drill sites and where temperature profiles are available (Dome Fuji, Dome Concordia, Vostok and South Pole), are also retained. These are not the sites themselves, but zones of smaller ice thickness in their vicinity. Finally, suitable areas are found across the Gamburtsev Mountains and Ridge B
25 (between Dome Argus and Vostok). The former is characterized by a much larger spatial variability in bedrock topography, while the latter may suffer from a lack in decent constraints on ice thickness (according to Fig. 2 in Fretwell et al., 2013).

2873

Subglacial topography is a key factor in determining suitable sites for oldest ice. Given the strong relationship between basal temperatures and ice thickness, as depicted by Fig. 1, it is quite likely to find suitable cold-based spots in the vicinity of deep ice core sites that have the bottom ice at or near pressure melting point. Areas that
5 should be avoided are those in which a large number of subglacial lakes are found, such as the Lakes District, where even low values of GHF are sufficient to keep the ice at pressure melting.

Another factor that may influence basal conditions is due to the glacial-interglacial history of the ice sheet and the time-scales needed for the ice sheet to thermally adapt
10 to different climates. Moreover, the temperature calculations made in this study are based on present-day observed parameters of surface temperature, ice thickness and accumulation rate. To test this effect, we calculated the minimum geothermal heat flow G_{min} needed to keep the base at pressure melting point for environmental conditions that are the mean for a longer time span. We reduced the surface temperature T_s by
15 6 K, reduced the surface accumulation rate \dot{a} to 60 % of its current value, and reduced ice thickness H with 100 m, which is valid for the divide areas. The results are surprisingly coherent with the previously-calculated values, and are therefore not shown separately. The main reason is that for this spread of values the reduced accumulation rate (which reduces vertical advection, hence warms the bottom ice layers) is largely
20 counteracted by the decrease in surface temperature. However, one needs to keep in mind that both calculations (present-day and mean glacial-interglacial) relate to steady-state conditions, which in reality is not the case.

Nevertheless, one should be careful in using the above model results as a sole guide in the process of detecting suitable cold-based areas for retrieving a long ice-core record, due to a number of factors that were not taken into account:
25

1. Areas characterized by subglacial mountains or other bedrock variability may well be suitable from a thermal point of view, the topographic variability may well hamper the deciphering of the climate signal due to complex processes, such as ice overturning (NEEM community members, 2013) or refreezing (Bell et al., 2011).

2874

2. The upper limit on the flow velocity of 2 myr^{-1} may also be too high for reconstructing the climate signal without having to rely too heavily on ice flow models for correcting for upstream advection. In theory, ice could have traveled over several hundreds of kilometers before reaching the ice core site, and this without taking into account any shifts in ice divides over glacial-interglacial periods, which would also influence the flow direction over time.
3. The spatial variability of GHF may in reality be much higher than the one represented in the three GHF datasets.
4. Areas where bedrock data is unavailable (or where interpolation is based on sparse data) may be wrongly classified in the above analysis, and some suitable areas thus overseen.

While this paper gives an overview of continental-scale basal conditions of the Antarctic ice sheet, the processed datasets from both the simple (\bar{G} , σ_G) and the full model (\bar{T} , RMSE_T) will be made available online together with simple MatLab scripts to allow for a more detailed search/zoom for potential sites, based on the figures presented here.

Acknowledgements. This paper forms a contribution to the FNRS–FRFC project (Fonds de la Recherche Scientifique) entitled “NEEM: The Eemian and beyond in Greenland ice”. The authors are indebted to C. Ritz for valuable discussions and commenting on an earlier version of the manuscript.

2875

References

- Bell, R. E., Studinger, M., Fahnestock, M. A., and Shuman, C. A.: Tectonically controlled subglacial lakes on the flanks of the Gamburtsev Subglacial Mountains, East Antarctica, *Geophys. Res. Letters*, **33**, L02504, doi:10.1029/2005GL025207, 2006. 2871
- Bell, R. E., Studinger, M., Fahnestock, M. A., and Joughin, I.: Large subglacial lakes in East Antarctica at the onset of fast-flowing ice streams, *Nature*, **445**, 904–907, doi:10.1038/nature05554, 2007. 2871
- Bell, R. E., Ferraccioli, F., Creyts, T. T., Braaten, D., Corr, H., Das, I., Damaske, D., Frearson, N., Jordan, T., Rose, K., Studinger, M., and Wolovick, M.: Widespread persistent thickening of the East Antarctic ice sheet by freezing from the base, *Science*, **331**, 1592–1595, 2011. 2867, 2874
- Budd, W. F. and Warner, R. C.: A computer scheme for rapid calculations of balance–flux distributions, *Ann. Glaciol.*, **23**, 21–27, 1996. 2864
- Carter, S. P., Blankenship, D. D., Peters, M. F., Young, D. A., Holt, J. W., and Morse, D. L.: Radar-based subglacial lake classification in Antarctica, *Geochem. Geophys. Geosys.*, **8**, Q03016, doi:10.1029/2006GC001408, 2007. 2871
- Dahl-Jensen, D., Morgan, V. I., and Elcheikh, A.: Monte Carlo inverse modelling of the Law Dome (Antarctica) temperature profile, *Ann. Glaciol.*, **29**, 145–150, 1999. 2870
- DeConto, R. M. and Pollard, D.: Rapid Cenozoic glaciation of Antarctica induced by declining atmospheric CO_2 , *Nature*, **421**, 245–249, 2003. 2861
- EPICA community members: Eight glacial cycles from an Antarctic ice core, *Nature*, **429**, 623–628, 2004. 2861
- EPICA community members: One-to-one coupling of glacial climate variability in Greenland and Antarctica, *Nature*, **444**, 195–198, 2006. 2861
- Fox-Maule, C., Purucker, M. E., Olsen, N., and Mosegaard, K.: Heat flux anomalies in Antarctica revealed by satellite magnetic data, *Science*, **309**, 464–467, 2005. 2865, 2871, 2882
- Fretwell, P., Pritchard, H. D., Vaughan, D. G., Bamber, J. L., Barrand, N. E., Bell, R., Bianchi, C., Bingham, R. G., Blankenship, D. D., Casassa, G., Catania, G., Callens, D., Conway, H., Cook, A. J., Corr, H. F. J., Damaske, D., Damm, V., Ferraccioli, F., Forsberg, R., Fujita, S., Gim, Y., Gogineni, P., Griggs, J. A., Hindmarsh, R. C. A., Holmlund, P., Holt, J. W., Jacobel, R. W., Jenkins, A., Jokat, W., Jordan, T., King, E. C., Kohler, J., Krabill, W., Riger-Kusk, M., Langley, K. A., Leitchenkov, G., Leuschen, C., Luyendyk, B. P., Matsuoka, K.,

2876

- Mouginot, J., Nitsche, F. O., Nogi, Y., Nost, O. A., Popov, S. V., Rignot, E., Rippin, D. M., Rivera, A., Roberts, J., Ross, N., Siegert, M. J., Smith, A. M., Steinhage, D., Studinger, M., Sun, B., Tinto, B. K., Welch, B. C., Wilson, D., Young, D. A., Xiangbin, C., and Zirizzotti, A.: Bedmap2: improved ice bed, surface and thickness datasets for Antarctica, *The Cryosphere*, 7, 375–393, doi:10.5194/tc-7-375-2013, 2013. 2864, 2873
- 5 Fricker, H. A. and Scambos, T.: Connected subglacial lake activity on lower Mercer and Whillans Ice Streams, West Antarctica, 2003–2008, *J. Glaciol.*, 55, 303–315, 2009. 2871
- Fricker, H. A., Warner, R., and Allison, I.: Mass balance of the Lambert Glacier-Amery Ice Shelf system, East Antarctica: a comparison of computed balance fluxes and measured fluxes, *J. Glaciol.*, 46, 561–570, 2000. 2864
- 10 Fricker, H. A., Scambos, T., Bindschadler, R., and Padman, L.: An active subglacial water system in West Antarctica mapped from space, *Science*, 315, 1544–1548, doi:10.1126/science.1136897, 2007. 2871
- Fujii, Y., Azuma, N., Tanaka, Y., Nakayama, M., Kameda, T., Shinbori, K., Katagiri, K., Fujita, S., Takahashi, A., Kawada, K., Motoyama, H., Narita, H., Kamiyama, K., Furukawa, T., 15 Takahashi, S., Shoji, H., Enomoto, H., Sitoh, T., Miyahara, T., Naruse, R., Hondoh, T., Shiraiwa, T., Yokoyama, K., Ageta, Y., Saito, T., and Watanabe, O.: Deep ice core drilling to 2503 m depth at Dome Fuji, Antarctica, *Mem. Natl Inst. Polar Res., Spec. Issue*, 56, 103–116, 2002. 2870
- 20 Gow, A. J., Ueda, H. T., and Garfield, D. E.: Antarctic ice sheet – preliminary results of first core hole to bedrock, *Science*, 161, 1011–1013, 1968. 2870
- Grotes, P. M., Stuiver, M., White, J. W. C., Johnson, S., and Jouzel, J.: Comparison of oxygen isotope records from the GISP2 and GRIP Greenland ice cores, *Nature*, 366, 552–554, 1993. 2867
- 25 Hindmarsh, R. C. A.: On the numerical computation of temperature in an ice sheet, *J. Glaciol.*, 45, 568–574, 1999. 2862, 2863, 2869
- Hindmarsh, R. C. A., Leysinger Vieli, G. J. M. C., and Parrenin, F.: A large-scale numerical model for computing isochrone geometry, *Ann. Glaciol.*, 50, 130–140, 2009. 2869
- Hondoh, T., Shoji, H., Watanabe, O., Salamatin, A. N., and Lipenkov, V.: Depth-age and temperature prediction at Dome Fuji Station, East Antarctica, *Ann. Glaciol.*, 35, 384–390, 2002. 2870
- 30 Hutter, K.: *Theoretical Glaciology*, Kluwer Academic Publishers, Dordrecht, 1983. 2869

2877

- Johnson, S.: Oxygen isotope and palaeotemperature records from six Greenland ice-core stations: Camp Century, Dye-3, GRIP, GISP2, Renland and NorthGRIP, *J. Quaternary Sci.*, 16, 299–307, 2001. 2861
- Jouzel, J. and Masson-Delmotte, V.: Deep ice cores: the need for going back in time, *Quaternary Sci. Rev.*, 29, 3683–3689, 2010. 2860, 2861
- 5 Le Brocq, A. M., Payne, A. J., and Siegert, M. J.: West Antarctic balance calculations: impact of flux-routing algorithm, smoothing algorithm and topography, *Comput. Geosci.*, 32, 1780–1795, 2006. 2864
- Lisiecki, L. E. and Raymo, M. E.: A Pliocene-Pleistocene stack of 57 globally distributed benthic $\delta^{18}\text{O}$ records, *Paleoceanography*, 20, PA1003, doi:10.1029/2004PA001071, 2005. 2861
- 10 L uthi, D., Lefloch, M., Bereiter, B., Blunier, T., Barnola, J. M., Siegenthaler, U., Raynaud, D., Jouzel, J., Fischer, H., Kawamura, K., and Stocker, T. F.: High-resolution carbon dioxide concentration record 650 000–800 000 years before present, *Nature*, 453, 379–382, 2008. 2860
- 15 MacGregor, J. A., Winebrenner, D. P., Conway, H., Matsuoka, K., Mayewski, P. A., and Clow, G. D.: Modeling englacial radar attenuation at Siple Dome, West Antarctica, using ice chemistry and temperature data, *J. Geophys. Res.*, 112, F03008, doi:10.1029/2006JF000717, 2007. 2870
- NEEM community members: Eemian interglacial reconstructed from a Greenland folded ice core, *Nature*, 493, 489–494, 2013. 2861, 2874
- 20 Parrenin, F., Remy, F., Ritz, C., Siegert, M., and Jouzel, J.: New modelling of the Vostok ice flow line and implication for the glaciological chronology of the Vostok ice core, *J. Geophys. Res.*, 109, D20102, doi:10.1029/2004JD004561, 2004. 2870
- Parrenin, F., Dreyfus, G., Durand, G., Fujita, S., Gagliardini, O., Gillet, F., Jouzel, J., Kawamura, K., Lhomme, N., Masson-Delmotte, V., Ritz, C., Schwander, J., Shoji, H., Uemura, R., Watanabe, O., and Yoshida, N.: 1-D-ice flow modelling at EPICA Dome C and Dome Fuji, East Antarctica, *Clim. Past*, 3, 243–259, doi:10.5194/cp-3-243-2007, 2007. 2870
- 25 Pattyn, F.: A new 3-D higher-order thermomechanical ice-sheet model: basic sensitivity, ice-stream development and ice flow across subglacial lakes, *J. Geophys. Res.*, 108, 2382, doi:10.1029/2002JB002329, 2003. 2868
- 30 Pattyn, F.: Antarctic subglacial conditions inferred from a hybrid ice sheet/ice stream model, *Earth Planet. Sc. Lett.*, 295, 451–461, 2010. 2860, 2862, 2865, 2867, 2869, 2870

2878

- Pattyn, F.: Antarctic subglacial lake discharges, in: Antarctic Subglacial Aquatic Environments, edited by: Siegert, M. and Bindschadler, B., doi:10.1029/2010GM000935, AGU, Washington D.C., 2011. 2871
- Petit, J. R., Jouzel, J., Raynaud, D., Barkov, N. I., Barnola, J. M., Basile, I., Bender, M., Chappellaz, J., Davis, M., Delaygue, G., Delmotte, M., Kotlyakov, V., Legrand, M., Lipenkov, V. Y., Lorius, C., Pepin, L., Ritz, C., Saltzman, E., and Stievenard, M.: Climate and atmospheric history of the past 420 000 years from the Vostok ice core, Antarctica, *Nature*, 399, 429–436, 1999. 2861
- Pollard, D., DeConto, R. M., and Nyblade, A. A.: Sensitivity of Cenozoic Antarctic ice sheet variations to geothermal heat flux, *Global Planet. Change*, 49, 63–74, 2005. 2862
- Popov, S. V. and Masolov, V. N.: Forty-seven new subglacial lakes in the 0–110° sector of East Antarctica, *J. Glaciol.*, 53, 289–297, 2007. 2871
- Price, P. B., Nagornov, O. V., Bay, R., Chirkin, D., He, Y., Miocinovic, P., Richards, A., Woschnagg, K., Koci, B., and Zagorodnov, V.: Temperature profile for glacial ice at the South Pole: implications for life in a nearby subglacial lake, *P. Natl. Acad. Sci. USA*, 99, 7844–7847, 2002. 2870
- Puruker, M.: Geothermal heat flux data set based on low resolution observations collected by the CHAMP satellite between 2000 and 2010, and produced from the MF-6 model following the technique described in Fox Maule et al. (2005), available at: <http://websrv.cs.umd.edu/isis/index.php>, last access: 23 March 2013. 2865, 2872, 2882
- Rial, J. A., Oh, J., and Reischmann, E.: Synchronization of the climate system to eccentricity forcing and the 100 000-year problem, *Nat. Geosci.*, 6, 289–293, 2013. 2861
- Rignot, E., Mouginot, J., and Scheuchl, B.: Ice flow of the antarctic ice sheet, *Science*, 333, 1427–1430, 2011. 2868
- Ritz, C.: Time Dependent Boundary Conditions for Calculation of Temperature Fields in Ice Sheets, *IAHS Publ.*, 170, 207–216, 1987. 2869
- Ruth, U., Barnola, J.-M., Beer, J., Bigler, M., Blunier, T., Castellano, E., Fischer, H., Fundel, F., Huybrechts, P., Kaufmann, P., Kipfstuhl, S., Lambrecht, A., Morganti, A., Oerter, H., Parrenin, F., Rybak, O., Severi, M., Udisti, R., Wilhelms, F., and Wolff, E.: “EDML1”: a chronology for the EPICA deep ice core from Dronning Maud Land, Antarctica, over the last 150 000 years, *Clim. Past*, 3, 475–484, doi:10.5194/cp-3-475-2007, 2007. 2870

2879

- Salamatin, A. N., Lipenkov, V. Y., and Blinov, K. V.: Vostok (Antarctica) climate record time-scale deduced from the analysis of a borehole-temperature profile, *Ann. Glaciol.*, 20, 207–214, 1994. 2870
- Shapiro, N. M. and Ritzwoller, M. H.: Inferring surface heat flux distributions guided by a global seismic model: particular application to Antarctica, *Earth Planet. Sc. Lett.*, 223, 213–224, 2004. 2862, 2865, 2866, 2871, 2882
- Siegert, M. J.: Antarctic subglacial lakes, *Earth-Sci. Rev.*, 50, 29–50, 2000. 2862
- Siegert, M. J., Carter, S., Tobacco, I., Popov, S., and Blankenship, D.: A revised inventory of Antarctic subglacial lakes, *Antarct. Sci.*, 17, 453–460, 2005. 2871
- Smith, B. E., Fricker, H. A., Joughin, I. R., and Tulaczyk, S.: An inventory of active subglacial lakes in Antarctica detected by ICESat (2003–2008), *J. Glaciol.*, 55, 573–595, 2009. 2862, 2871
- van de Berg, W. J., van den Broeke, M. R., Reijmer, C. H., and van Meijgaard, E.: Reassessment of the Antarctic surface mass balance using calibrated output of a regional atmospheric climate model, *J. Geophys. Res.*, 111, D11104, doi:10.1029/2005JD006495, 2006. 2864
- van den Broeke, M. R.: Depth and density of the Antarctic firn layer, *Arct. Antarct. Alp. Res.*, 40, 432–438, 2008. 2864
- van den Broeke, M. R., van de Berg, W. J., and van Meijgaard, E.: Snowfall in coastal West Antarctica much greater than previously assumed, *Geophys. Res. Lett.*, 33, L02505, doi:10.1029/2005GL025239, 2006. 2864
- van Ommen, T. D., Morgan, V. I., Jacka, T. H., Woon, S., and Elcheikh, A.: Near-surface temperatures in the Dome Summit South (Law Dome, East Antarctica) borehole, *Ann. Glaciol.*, 29, 141–144, 1999. 2870
- Watanabe, O., Jouzel, J., Johnsen, S., Parrenin, F., Shoji, H., and Yoshida, N.: Homogeneous climate variability across East Antarctica over the past three glacial cycles, *Nature*, 422, 509–512, 2003. 2861
- Wright, A. P. and Siegert, M. J.: A fourth inventory of Antarctic subglacial lakes, *Antarct. Sci.*, 24, 659–664, 2012. 2862, 2871

2880

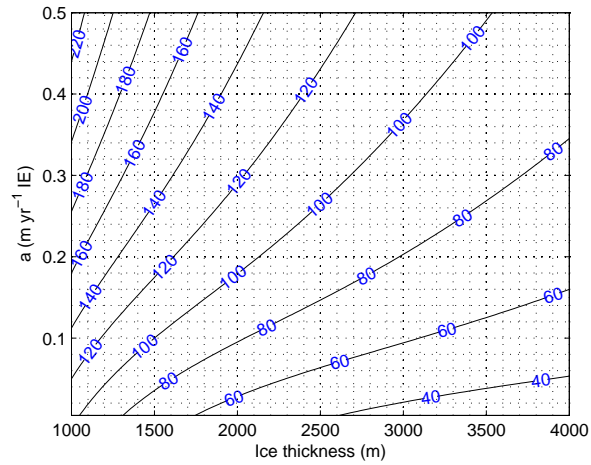


Fig. 1. Minimum GHF (mW m^{-2}) needed to keep the bed at pressure melting point as a function of surface accumulation rate (ice equivalent, IE) and ice thickness and in the absence of horizontal advection. Results are shown for a mean surface temperature of $T_s = -50^\circ\text{C}$.

2881

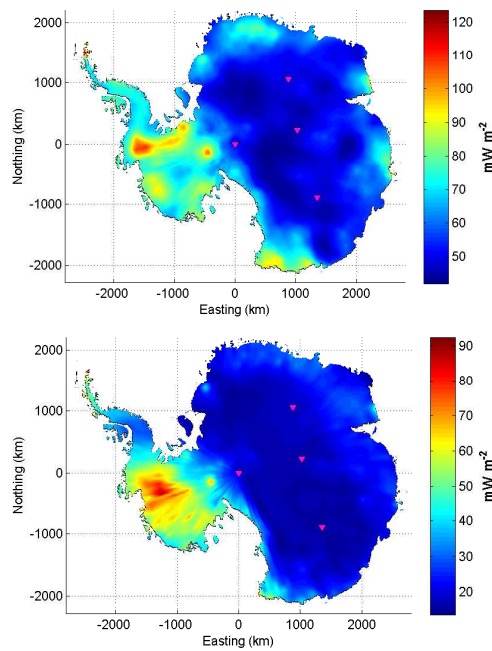


Fig. 2. Top: mean GHF \bar{G} (mW m^{-2}) based on GHF estimates by Puruker (2013), Fox-Maule et al. (2005) and Shapiro and Ritzwoller (2004). Bottom: standard deviation σ_G on the GHF datasets. The magenta triangles are the major drill site (from top to bottom): Dome Fuji, Dome Argus, South Pole and Dome Concordia.

2882

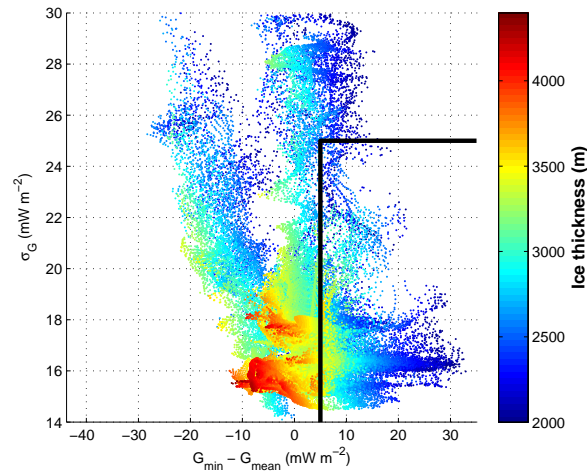


Fig. 3. Scatterplot of $\Delta G = G_{\min} - \bar{G}$ versus σ_G for all points with ice thickness $H > 2000$ m and horizontal flow speed $< 2 \text{ m yr}^{-1}$. The colorscale depicts ice thickness for each of the grid points. Negative values of ΔG means that pressure melting point is reached, hence basal melt occurs. Positive values means that the minimum required heat flow to reach pressure melting point is higher than the mean of the three GHF datasets. Points lying within the rectangle are likely to be cold based, taken into account the variability of GHF.

2883

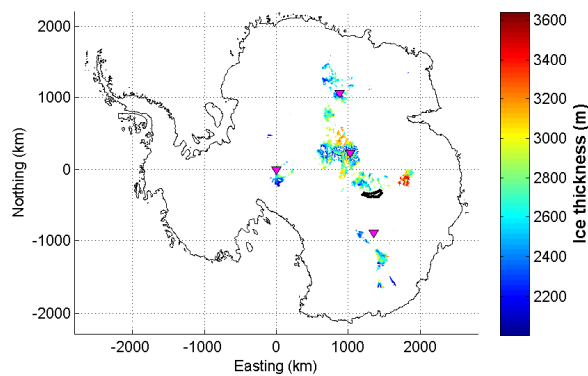


Fig. 4. Potential locations of cold basal conditions in areas with ice thickness $H > 2000$ m (colorbar) and horizontal flow speeds smaller than 2 m yr^{-1} , for $\Delta G < 10 \text{ mW m}^{-2}$ and $\sigma_G < 10 \text{ mW m}^{-2}$, and as calculated with the simple model.

2884

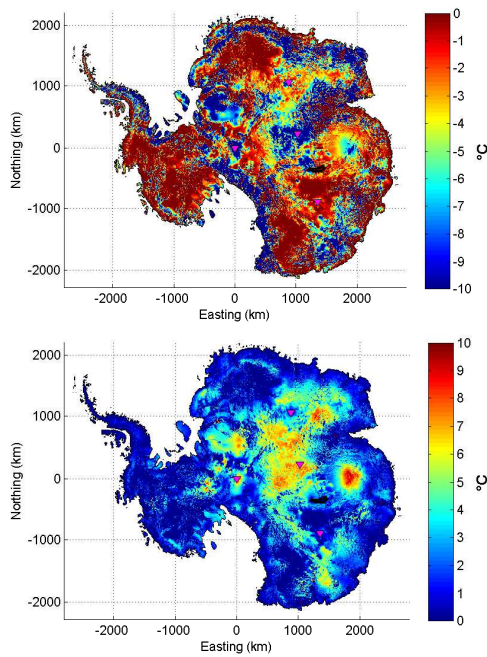


Fig. 5. Top: mean temperature according to the ensemble of 15 experiments (see text for more details), corrected for the dependence on pressure. The lower limit has been cut of at -10°C . Bottom: Root Mean Square Error (RMSE, $^{\circ}\text{C}$) according to the same ensemble.

2885

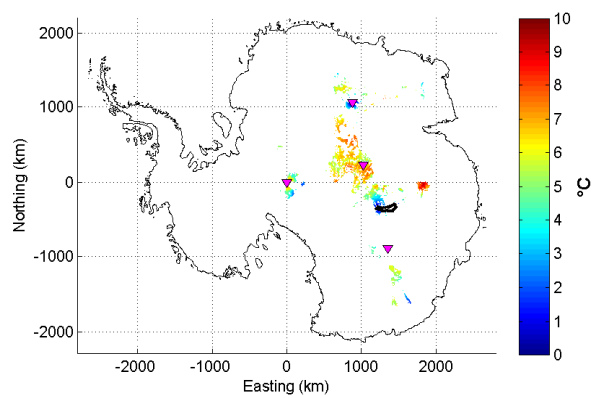


Fig. 6. Potential locations of cold basal conditions in areas with ice thickness $H > 2000\text{ m}$, horizontal flow speeds are smaller than 2 myr^{-1} and basal temperatures as calculated with the full model are lower than -5°C . The colorbar denotes the RMSE ($^{\circ}\text{C}$) based on the ensemble calculations.

2886

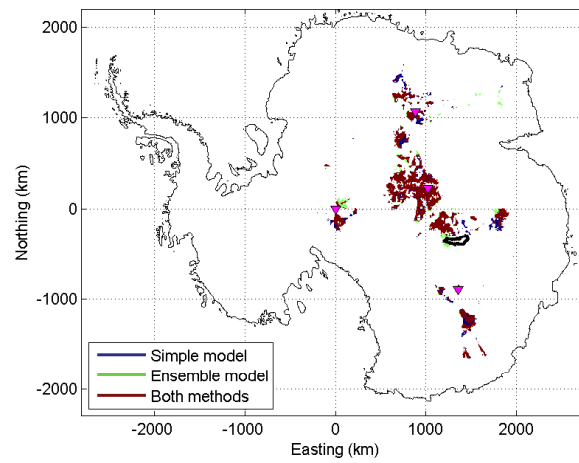


Fig. 7. Potential locations of cold basal conditions in areas with ice thickness $H > 2000$ m, horizontal flow speeds are smaller than 2 myr^{-1} according to the simple model (depicted in Fig. 4) and the ensemble model (depicted in Fig. 6).